PHYSICAL REVIEW B VOLUME 50, NUMBER 8 15 AUGUST 1994-II

Anisotropic optical properties of an oriented-emeraldine-base polymer and an emeraldine-hydrochloride-salt polymer

R. P. McCall
Department of Physics, Louisiana Tech University, Ruston, Louisiana 71272

E. M. Scherr and A. G. MacDiarmid
Department of Chemistry, University of Pennsylvania, Philadelphia, Pennsylvania 19104

A. J. Epstein
Departments of Physics and Chemistry, The Ohio State University, Columbus, Ohio 43210

(Received 3 February 1994)

We present results of polarized reflectance measurements for unstretched and stretched films of polyaniline in the insulating emeraldine-base (EB) and conducting emeraldine-salt (ES) forms. The reflectance data and the resulting optical conductivity, obtained from a Kramers-Kronig transform of the reflectance data, of unstretched films agree well with optical data reported by S. Stafström *et al.* [Phys. Rev. Lett. **59**, 1464 (1987)]. The stretched films (400% elongation) show significant anisotropy in the reflectance and the other optical constants. The frequency-dependent conductivity in ES exhibits a large shift in oscillator strength to lower energies compared to that of EB and compared to that of unstretched films of ES, which demonstrates delocalization of conduction electrons in the "polaron band." The dielectric constant of stretched ES indicates that ES is metal-like, with maximum conductivity greater than ten times the dc conductivity. These results indicate that the dc conductivity is likely dominated by interchain processes and that higher values for conductivity are possible.

I. INTRODUCTION

Polyaniline is a family of conducting polymers that has been the subject of a large number of experimental and theoretical studies in the last few years.[1] This family of polymers exhibits a wide range of electronic, optical, magnetic, and mechanical properties that have made possible an increasing number of important technological applications. The variety of materials in this family results from the variation of the number of protons and the number of electrons on the polymer backbone. Other members have been synthesized through derivatization of the parent polymer by the addition of methyl, ethyl, methoxy, sulfonic, or other groups.[2]

Many of the properties of polyaniline result from the nature of the polymer backbone, which consists of alternating C_6 rings and nitrogen heteroatoms in either the amine (N-H) or imine (N only) form, Fig. 1. It has been demonstrated[2] that polyaniline may be prepared in three discrete oxidation states: the fully reduced leucoemeraldine base (LEB), the half-oxidized emeraldine base (EB), and the fully oxidized pernigraniline base (PNB). Each of these forms of polyaniline is an insulator and possesses other interesting physical and chemical properties.

Earlier studies[3,4] of the emeraldine form of polyaniline showed that the insulating emeraldine-base polymer can be doped with protonic acids, such as HCl, to obtain the emeraldine salt (ES) form, see Fig. 1(d), which has a dc conductivity of about 1 S/cm. The transport properties have been analyzed in terms of crystalline metallic regions with the conductivity limited by dc charge trans-

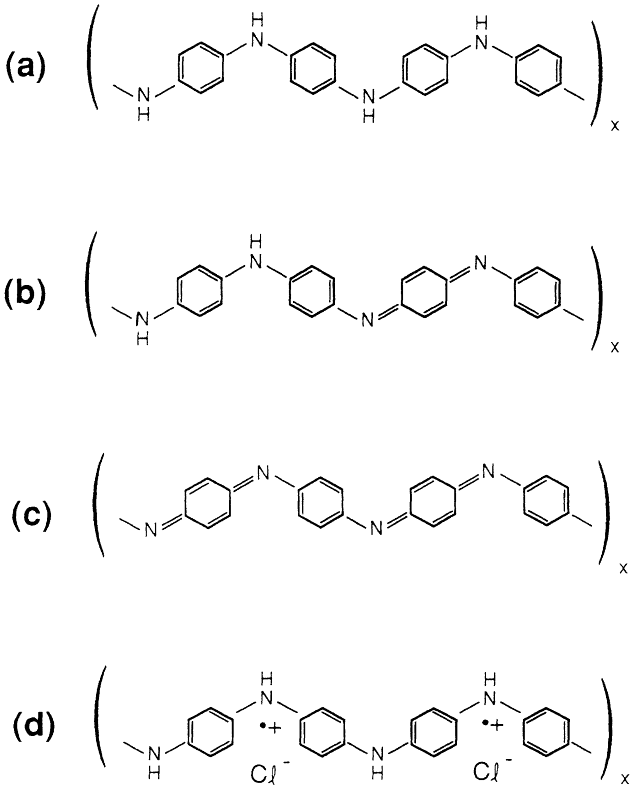

FIG. 1. Chemical structure of (a) leucoemeraldine base (LEB), (b) emeraldine base (EB), (c) pernigraniline base (PNB), and (d) emeraldine salt (ES).

port through the intervening disordered material.[5] The size and volume fraction of these crystalline regions vary with preparation technique, with typical values of 30–60 Å coherence lengths and 40–60 % crystallinity.[6] The conductivity results from the formation of a "polaron lattice" with a half occupied "polaron band."[7] This picture of polyaniline is supported by band-structure calculations,[8] as well as optical,[8] magnetic,[7] and transport[5] studies.

Emeraldine base is soluble in several solvents including *N*-methyl pyrrolidinone (NMP),[9–11] sulfuric acid,[12–14] 80% aqueous acetic acid, 60–88 % aqueous formic acid,[15] chloroform,[16] and *m*-cresol.[17,18] It has been shown that strong flexible films[9] and fibers[14,19] of EB and ES can be formed from solutions of NMP. Recently, it has been demonstrated[20] that films of emeraldine base that undergo simultaneous heat treatment and application of stress result in oriented, partially crystalline polyaniline films. Elongations of up to 450% or higher have been achieved. The stretched EB film can be doped with HCl to obtain stretch-oriented emeraldine salt films. The polymers exhibit anisotropic behavior in their tensile strength, x-ray diffraction pattern, and ac and dc conductivities.[20]

Polarized infrared absorption studies[20] of stretched films of emeraldine base show significant anisotropy for light polarized parallel and perpendicular to the orientation direction. The major infrared modes at 1150, 1300, 1500, and 1600 cm^{-1} exhibit increasing anisotropy with increasing elongation for *parallel* polarization, which is consistent with their orientation parallel to the polymer axis (*c* axis). The ir mode at 850 cm^{-1} shows increasing anisotropy with increasing elongation for *perpendicular* polarization, consistent with its orientation perpendicular to the C_6 rings. Analysis of the dichroic ratio of the integrated oscillator strength for each mode in the parallel and perpendicular polarizations indicates that the plane of the C_6 rings makes an angle of $56°\pm 15°$ with respect to the plane of the nitrogen atoms. This prediction is in reasonable agreement with the ring torsion angle of about 30° determined by analysis of x-ray diffraction patterns of emeraldine base.[6]

Earlier optical experiments[20,21] reveal significant anisotropy in the reflectance for parallel and perpendicular polarizations of visible and ultraviolet light. However, these experiments did not present the anisotropic behavior of other optical constants such as optical conductivity, dielectric constant, index of refraction, and extinction coefficient. In this paper, we report measurements of the reflectance of unstretched and stretched emeraldine base and emeraldine salt, in addition to anisotropy observed in optical constants obtained by Kramers-Kronig transform of the reflectance data. These results indicate that emeraldine base is an insulator with optical transitions at approximately 2.0, 3.7, and 6.2 eV, which is consistent with direct absorption measurements of solutions of EB. For solutions and for modestly conducting films of emeraldine salt, there is a significant shift of the conductivity peak at 1.5 eV, which is associated with isolated polarons, to lower energies for light polarized perpendicular to the chain. An even larger shift occurs for light polarized parallel to the chain. These data support the delocalization of conduction electrons in the "polaron band" to form a metallic state in well-prepared samples.

In the next section of this paper, we describe the experimental techniques used in this study, including a discussion of the Kramers-Kronig calculation used to determine the optical constants. In Sec. III, we present and discuss the experimental results for the reflectance measurements of stretched EB, stretched ES, and unstretched ES, in addition to the results for the optical constants. We summarize our results in the final section.

II. EXPERIMENTAL TECHNIQUES

A. Sample preparation

Samples of amorphous emeraldine-base powder, classified as EB-I,[6] were prepared using previously described methods.[22,23] Enough EB powder was dissolved in NMP to produce a 2% (by weight) solution. Films of partially crystalline EB-II, were prepared by first pouring this solution onto glass plates, then placing these plates in a vacuum oven at about 50 °C for about 24 h. After most of the NMP was driven off, a high-quality film remained, which was then removed from the glass plate by immersion in distilled water. These films, which are flexible and copper colored, are about 10–50 μm thick and contain up to 20% by weight NMP. The NMP acts as a plasticizer, which lowers the glass transition temperature T_g.[24]

The EB films are stretched by heating them to temperatures above T_g while maintaining the sample under a uniaxial stress. Films with elongation of up to 450% ($l/l_0=4.5$) can be achieved using this process. Stretched and unstretched films of ES were obtained by equilibrating stretched and unstretched films of EB in 1.0 M HCl for 48–60 h. Because this method of doping typically causes the films to curl and become quite brittle, a Teflon sample holder was designed to keep the films under slight tension during the doping process. This sample holder was also used to hold the samples flat during the optical reflectance measurements.

B. Reflectance measurements

The polarized and unpolarized reflectance spectra of stretched and unstretched films of EB and ES were measured with two instruments: a Perkin-Elmer Lambda 19 UV/Vis/NIR spectrophotometer and a Nicolet 60SX Fourier transform infrared (FTIR) spectrometer. Measurements using the UV/Vis/NIR spectrophotometer ranged from 0.56 to 6.5 eV (2200 to 190 nm, or 4500 to 52 600 cm^{-1}), while those obtained with the FTIR spectrometer ranged from 0.062 to 1.2 eV (20 μm to 1000 nm, or 500 to 10 000 cm^{-1}). For the polarized measurements, a wire grid polarizer was used in the far- to near- ir, and dichroic film polarizers were used in the near ir to near uv, in addition to a Glan-Taylor polarizing prism.

Although the polymer films were quite flat, a small amount of diffuse scattering was evident. To correct for this, reflectance measurements using the UV/Vis/NIR spectrophotometer were made with an integrating sphere.

This method allowed for direct determination of the absolute reflectance without having to correct for scattering by the usual method of coating the sample with gold or aluminum. Because Spectralon is used as the reference surface inside the integrating sphere, the reflectivity of the samples is corrected for the reflectivity of Spectralon. Spectra obtained with the FTIR spectrometer were measured with respect to aluminum mirrors, and subsequently corrected for the reflectivity of aluminum. The FTIR spectra closely matched that from the UV/Vis/NIR instrument, which indicated that there was little diffuse reflectance from the samples.

C. Kramers-Kronig calculation

Because of the large frequency region covered by the reflectance measurements, a Kramers-Kronig (KK) analysis[25] of the reflectance provides quite accurate values for the optical constants of the polymer materials. In performing the KK analysis, conventional extrapolation procedures were used. For energies below 500 cm^{-1}, the reflectance was assumed to be constant. Between the highest frequency data point and 100 000 cm^{-1} (12.5 eV), the reflectance was assumed to fall off as $1/\omega^2$, whereas above 100 000 cm^{-1}, the extrapolation was taken as $1/\omega^4$. The Kramers-Kronig transform of the reflectance yields the phase shift on reflection. From the reflectance and the phase shift, the other optical constants, such as the conductivity, index of refraction, dielectric constant, absorption coefficient, and loss function can be determined.

III. RESULTS AND DISCUSSION

A. Emeraldine base

Previous direct-absorption measurements[26] in the near-infrared to ultraviolet region on solutions of emeraldine base reveal strong absorption bands centered at ~2.0 and ~3.8 eV. The higher-lying peak at 3.8 eV is attributed to the π-π^* band-gap absorption in agreement with theoretical calculations.[27] The absorption band at 2.0 eV results from an intrachain, charge-transfer, excitonlike transition from the highest occupied energy levels (centered on the benzenoid rings) to the lowest unoccupied energy level (centered on the quinoid rings).[7] Theoretical calculations[27–32] support this assignment.

The reflectance of 4×-stretched emeraldine base is shown in Fig. 2 for the electric field polarized parallel to the chain axis ($\mathbf{E}\|c$) and perpendicular to the chain axis ($\mathbf{E}\perp c$). Also shown is the reflectance of the same film with no polarizer in the beam path. Because the polarizers are not accurate above ~34 000 cm^{-1}, this measurement was useful to determine what other features are present at higher energies. The reflectance spectra show significant anisotropy for the parallel and perpendicular polarizations of the electric field.

Emeraldine base is quite transparent in the infrared so that interference (fringing) effects are measured in the spectra. In the FTIR spectrometer, these effects can be minimized somewhat by eliminating their signature in the interferogram before the Fourier transform is performed. In the UV/Vis/NIR spectrophotometer, elimination of the interference fringes was not possible, the fringes can be observed in the spectra near 6000 cm^{-1}, particularly in the $\mathbf{E}\perp c$ spectrum. These features do not alter the overall results by a significant amount, although at low energies they do cause slight complications in interpreting the results.

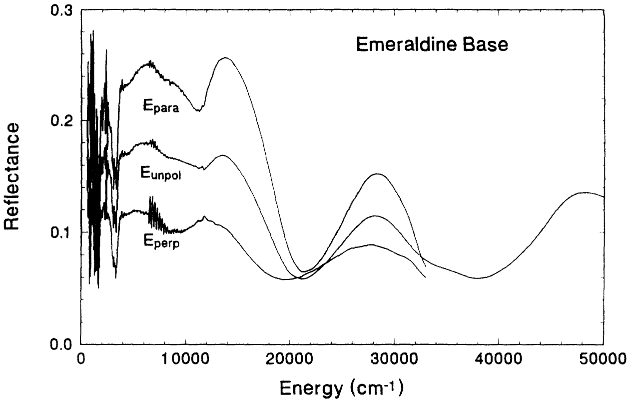

FIG. 2. Reflectance of 4×-stretched emeraldine base for the electric field polarized parallel to the chain axis ($\mathbf{E}\|c$) and perpendicular to the chain axis ($\mathbf{E}\perp c$), and for no polarizer in the beam path $\mathbf{E}_{\mathrm{unpol}}$.

Plots of the frequency-dependent absorption coefficient $\alpha(\omega)$ of EB for $\mathbf{E}\|c$, for $\mathbf{E}\perp c$, and for no polarizer are shown in Fig. 3. The maxima in $\alpha(\omega)$ near 16 000 cm^{-1} (2.0 eV) and at 28 000–30 000 cm^{-1} (3.5–3.7 eV) correspond to the electronic transitions previously observed and discussed for solutions of emeraldine base.[26] The exciton peak at 2 eV shows the most anisotropy, being much stronger for the parallel polarization than for the perpendicular polarization. This result is consistent with its assignment as an excitonlike transition involving intrachain charge transfer from the benzenoid rings to the quinoid rings. The absorption peak at 50 000 cm^{-1} (6.2 eV) corresponds to transitions from lower-lying energy bands to the conduction band.[30] It is interesting to note the presence of the small peak at ~35 000 cm^{-1} (4.3 eV) in the unpolarized spectrum, which is attributed to the

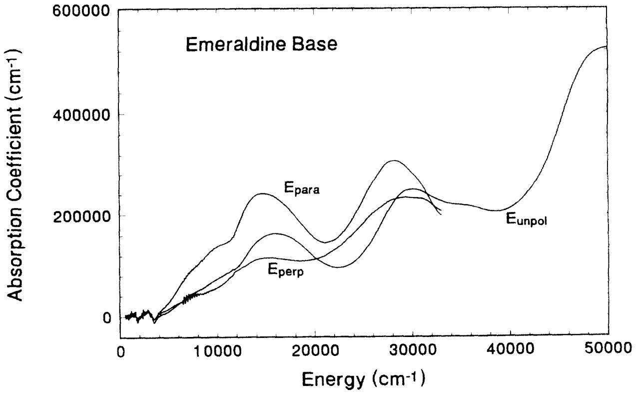

FIG. 3. Frequency-dependent absorption coefficient of emeraldine base obtained from Kramers-Kronig transform of the reflectance data of Fig. 2.

π-π^* band-gap absorption centered on the quinoid rings.[32–34] Typically, this peak is not observed in solutions of emeraldine base, but rather in solutions of pernigraniline base.[34] The presence of this peak suggests that the EB films studied may have an excess of quinoid rings, i.e., they are slightly overoxidized.

B. Emeraldine salt

Upon protonation of the emeraldine base to the conducting emeraldine salt, direct-absorption measurements[35] on solutions of emeraldine salt reveal dramatic changes in the spectrum. The 2-eV absorption of emeraldine base disappears, and is replaced in emeraldine salt by strong absorptions centered at about 1.4 and 3.0 eV. These absorptions arise due to the formation of a polaron band during protonation. The presence of the polaron band allows for new transitions from lower-lying bands that occur at the specified energies.[8] This model is supported by reflectance measurements by Stafström *et al.* on films of unstretched emeraldine salt.

For 4×-stretched films of emeraldine salt, the dc conductivity parallel to the stretching direction is approximately 3–4 times larger than that perpendicular to the stretching direction,[20] with absolute conductivities parallel to the stretching direction reported as high as 300 S/cm.[5] The samples used in the reflectance measurements reported here had dc conductivities parallel to the stretching direction of $\sigma_{\parallel}=11.2$ S/cm and perpendicular to the stretching direction of $\sigma_{\perp}=2.6$ S/cm.

The reflectance of 4×-stretched films of emeraldine salt is shown in Fig. 4 for $\mathbf{E}\parallel c$ and for $\mathbf{E}\perp c$. In addition, because of the cutoff of the polarizers, measurements were extended to 50 000 cm^{-1} with no polarizer in the beam path to determine what effects occur at higher energies. Because ES is strongly absorbing, there are no interference effects observed in the spectra. There is significant anisotropy, with the parallel reflectance approaching values greater than 75% at low energies and the perpendicular reflectance remaining at or below 20%. Note that the reflectance spectrum for $\mathbf{E}\perp c$ is flatter in the visible region (14 000–25 000 cm^{-1}) than for $\mathbf{E}\parallel c$, which reflects more in the blue region than the red. This is consistent with what is observed when a stretched film of ES is examined through a visible polarizer; i.e., the perpendicular polarization appears more shiny or white in color than the parallel polarization, which appears dark blue.

The frequency-dependent absorption coefficient $\alpha(\omega)$ obtained from the Kramers-Kronig transform of the reflectance is shown in Fig. 5. For no polarizer in the beam path, there are four absorption peaks in ES near 9000 cm^{-1} (1.1 eV), 24 000 cm^{-1} (3.0 eV), 31 000 cm^{-1} (3.8 eV), and 50 000 cm^{-1} (6.2 eV). For the $\mathbf{E}\parallel c$ spectrum, the lower peak is shifted to about 6000 cm^{-1} (0.75 eV) and is quite weak in the $\mathbf{E}\perp c$ spectrum. At higher energies, both polarized results for the absorption coefficient give higher values than those for no polarizer. This is most likely due to extrapolation techniques of the reflectance, because for the two polarized reflectance measurements, extrapolation began at 32 000 cm^{-1}, which eliminates the additional information in the reflectance observed in the data with no polarizer in the beam path. The results do not significantly affect the shape or position of absorption peaks, but rather the overall level, particularly at higher energies.

Comparison of the absorption curve of ES film with that of ES in solution reveals important differences associated with the delocalization of the conduction electrons. Though the 3.0-eV absorption band remains essentially unchanged, the narrow band at 1.5 eV (assigned to polaron absorption in solution and observed as a relatively narrow peak in poorly conducting forms of emeraldine salt) has shifted substantially to lower energies. This result supports the polaron band model,[7,8] in which localization of isolated polarons on chains in solution gives the discrete absorption predicted for polarons.[36] Similar absorptions are observed for more poorly conducting film samples. The broadening and subsequent shift to lower energy of the 1.5-eV absorption, for the more highly conducting samples, supports the picture of an intrapolaron band, free-carrier-like absorption. The anisotropy of the

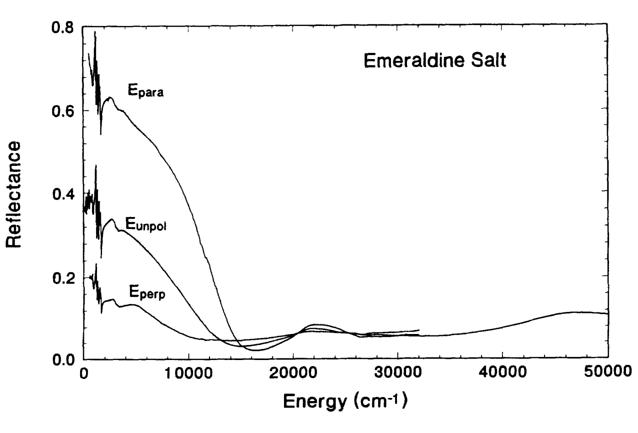

FIG. 4. Reflectance of 4×-stretched emeraldine salt for the electric field polarized parallel to the chain axis ($\mathbf{E}\parallel c$) and perpendicular to the chain axis ($\mathbf{E}\perp c$), and for no polarizer in the beam path $\mathbf{E}_{\text{unpol}}$.

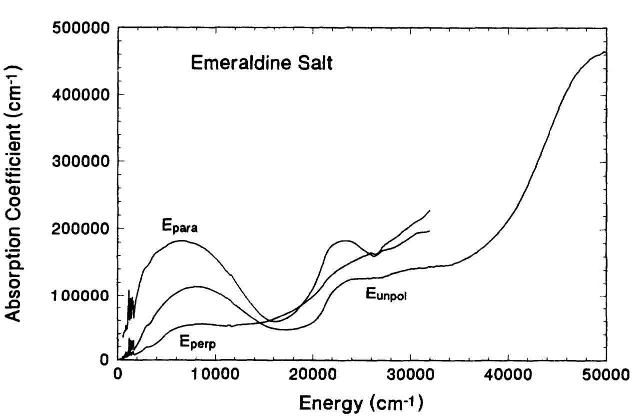

FIG. 5. Frequency-dependent absorption coefficient of 4×-stretched emeraldine salt obtained from Kramers-Kronig transform of the reflectance data of Fig. 4.

low-energy absorption for the 4×-stretched ES sample reveals that for these samples the extent of delocalization is different in parallel and perpendicular directions, in agreement with microwave frequency dielectric constant and conductivity measurements.[5] The infrared vibrational features in the range 1100–1600 cm^{-1} support previously reported results,[20] obtained using polarized direct-absorption spectroscopy, that show anisotropy for the parallel and perpendicular polarizations as mentioned in Sec. I.

The real part of the frequency-dependent conductivity $\sigma_1(\omega)$ is shown in Fig. 6. For no polarizer in the beam path, the conductivity data are similar to previously reported spectra on unstretched emeraldine salt,[8] although the peak near 11 000 cm^{-1} in that data is shifted to about 6 000 cm^{-1} for the stretched films. We have made reflectance measurements on unstretched films of ES which give conductivity data almost identical to that reported by Stafström *et al.*[8] Hence, similar to the absorption peak discussed above, the conductivity peak at 11 000 cm^{-1} in poorly conducting or solution samples of ES is shifted to lower energies for samples of higher conductivity. This result supports the increased delocalization of the electrons.

The frequency-dependent conductivities for parallel and perpendicular polarizations show significant anisotropy, Fig. 6. For $\mathbf{E}\parallel c$, there is a strong peak in conductivity near 2500 cm^{-1}, such a large shift in oscillator strength to lower energies occurs compared to results for unpolarized light and for unstretched films. This shift in oscillator strength is consistent with effective-medium-approximation calculations for a composite of small metal particles in an insulating host.[37] In these systems, for filling fractions f below the percolation threshold f_c, the conductivity shows a broad peak below the plasma frequency that shifts to lower energy as f approaches f_c. Above f_c, a Drude peak centered at zero frequency develops in addition to the broad absorption, giving a nonzero dc conductivity.

The conductivity data for no polarizer in the beam and for $\mathbf{E}\perp c$ both extrapolate to low values (approximately 1 S/cm) near dc, which agrees with dc conductivity measurements. However, the parallel polarization extrapolates to approximately 1000 S/cm at dc, which is two orders of magnitude higher than the measured value of $\sigma_{\parallel}=11.2$ S/cm. Thus, the measured dc value is likely dominated by interchain transport processes, and the intrinsic value of the conductivity has yet to be determined. This result is similar to that reported by Leising for metallic polyacetylene.[38]

The index of refraction n and the extinction coefficient k of 4×-stretched emeraldine salt for the electric field polarized parallel to the stretching direction are shown in Fig. 7(a). The index of refraction is quite high for low energies, falling to a value near $n=1$ at higher energies. The extinction coefficient falls below n to relatively low values for energies above approximately 13 000 cm^{-1}. For the perpendicular polarization, n ranges from 2–2.5 below 2000 cm^{-1} to 1.2–1.5 above 6000 cm^{-1}, whereas k is less than 1 for all energies measured, Fig. 7(b).

The real part of the dielectric function, determined by $\varepsilon_1=n^2-k^2$, and the imaginary part, determined by $\varepsilon_2=2nk$, for the parallel polarization of 4×-stretched emeraldine salt are shown in Fig. 8(a) and expanded by a factor of 10 in Fig. 9. The real part ε_1 is negative for the electric field polarized parallel to the chain direction for energies between 2000 and 12 600 cm^{-1} indicating nearly

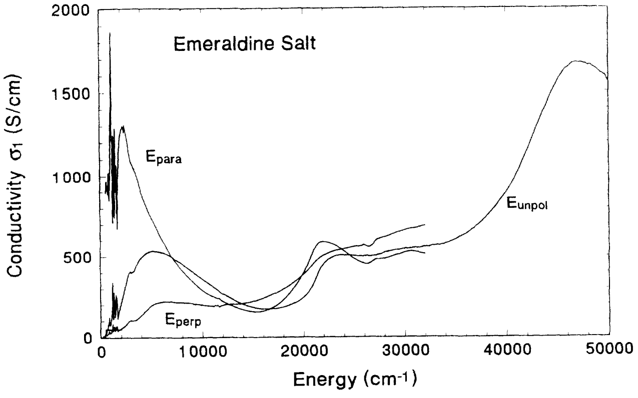

FIG. 6. Real part of the frequency-dependent conductivity $\sigma_1(\omega)$ of 4×-stretched emeraldine salt for the electric field polarized parallel to the chain axis ($\mathbf{E}\parallel c$) and perpendicular to the chain axis ($\mathbf{E}\perp c$), and for no polarizer in the beam path $\mathbf{E}_{\text{unpol}}$.

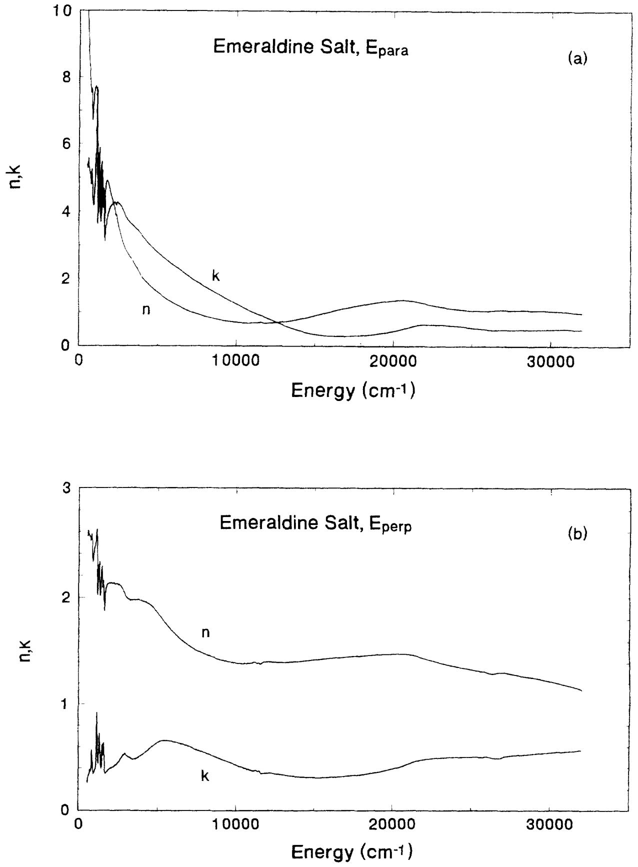

FIG. 7. The real and imaginary parts of the index of refraction, n and k, respectively, of 4×-stretched emeraldine salt for (a) $\mathbf{E}\parallel c$ and (b) $\mathbf{E}\perp c$.

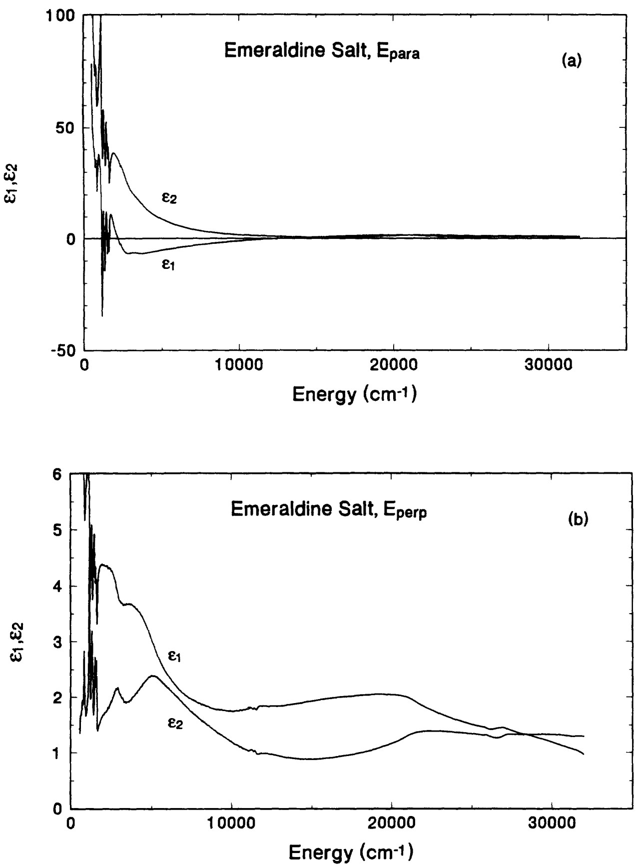

FIG. 8. The real and imaginary parts of the dielectric function, ε_1 and ε_2, of 4×-stretched emeraldine salt for (a) $\mathbf{E}\parallel c$ and (b) $\mathbf{E}\perp c$.

metallic behavior. At microwave frequencies (6×10^9 Hz, or 0.2 cm^{-1}) the dielectric constant of these samples is positive (~1000 at room temperature).[5] For the perpendicular polarization, the real part of the dielectric function is positive at all energies, Fig. 8(b), which is consistent with less electron delocalization in this direction.

From the dielectric function, the loss function can be calculated as

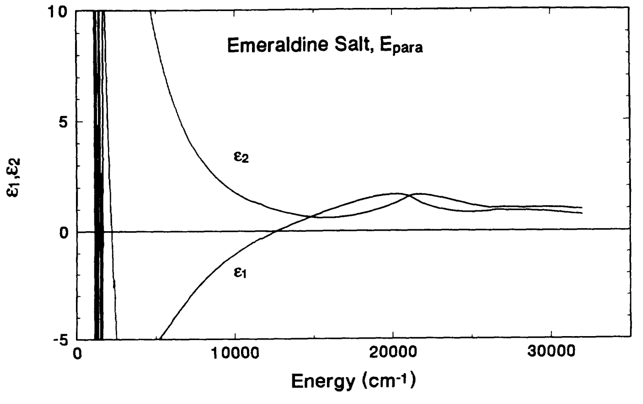

FIG. 9. The real and imaginary parts of the dielectric function, ε_1 and ε_2, of 4×-stretched emeraldine salt for $\mathbf{E}\parallel c$.

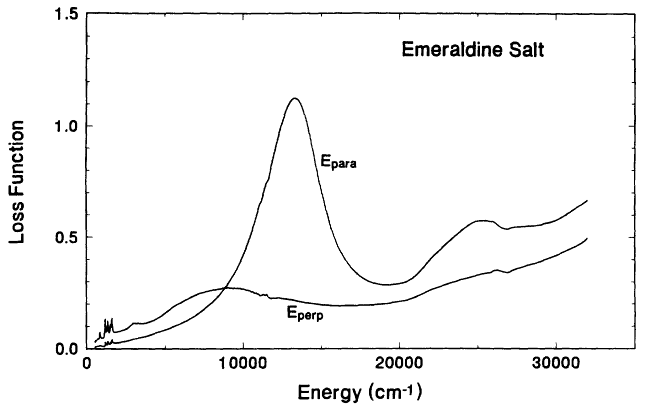

FIG. 10. The loss function of 4×-stretched emeraldine salt for $\mathbf{E}\parallel c$ and $\mathbf{E}\perp c$.

$$-\mathrm{Im}\,\varepsilon^{-1}=\frac{\varepsilon_2}{\varepsilon_1^2+\varepsilon_2^2}\ .$$

The loss function for emeraldine salt for the parallel polarization is shown in Fig. 10. A strong peak appears at approximately 13 200 cm^{-1} (1.64 eV). This value is close to the energy where $\varepsilon_1=\varepsilon_2$ at 14 600 cm^{-1} (1.81 eV), which is often taken as the position of the plasma energy E_p. In metallic polyacetylene,[38] Leising reports that the plasma energy is 3.51 eV consistent with higher values of E_p for better conductors. The loss function for the perpendicular direction, Fig. 10, does not show a well-defined maximum, reflecting an "over-damped" response. Hence, in the perpendicular direction, the electrons are less delocalized for these samples.

IV. SUMMARY

In summary, polarized reflectance measurements of stretched films of emeraldine base and emeraldine salt have revealed significant anisotropic features in their optical properties. The absorption coefficient of 4×-stretched films of emeraldine base shows that the excitonic transition near 2.0 eV is strongly polarized parallel to the chain axis, as expected. Results on emeraldine salt indicate that parallel to the chain axis, the polymer exhibits metal-like conductivity. This behavior causes a large shift of oscillator strength to lower energies with a large increase in conductivity expected. The much higher values for the frequency-dependent conductivity (about 1000 S/cm) compared to the dc conductivity (about 10 S/cm) indicate that the ultimate conductivities in these materials have not been attained, and that interchain transport processes dominate the dc transport.

ACKNOWLEDGMENTS

The authors wish to thank Gang Du for measuring the dc conductivities of the samples used in the reflectance measurements. This work was supported in part by the Defense Advanced Research Projects Agency through a contract monitored by the U. S. Office of Naval Research.

[1] See, for example *Proceedings of the International Conference on the Science and Technology of Synthetic Metals, Göteberg, Sweden, 1992* [Synth. Met. **55-57**, (1993)]; *Proceedings of the International Conference on the Science and Technology of Synthetic Metals, Tübingen, Germany, 1990* [Synth. Met. **41-43**, (1991)]; *Proceedings of the International Conference on the Science and Technology of Synthetic Metals, Santa Fe, New Mexico, 1988* [Synth. Met. **27** (1988) and **28,29** (1989)].

[2] A. G. MacDiarmid and A. J. Epstein, Chem. Soc. **88**, 317 (1989), and references therein.

[3] J. C. Chiang and A. G. MacDiarmid, Synth. Met. **13**, 193 (1986).

[4] A. G. MacDiarmid, J. C. Chiang, A. F. Richter, and A. J. Epstein, Synth. Met. **18**, 285 (1987).

[5] F. Zuo, M. Angelopoulos, A. G. MacDiarmid, and A. J. Epstein, Phys. Rev. B **36**, 3475 (1987); Z. H. Wang, H. H. S. Javadi, A. Ray, A. G. MacDiarmid, and A. J. Epstein, *ibid.* **42**, 5411 (1990); Z. H. Wang, A. Ray, A. G. MacDiarmid, and A. J. Epstein, *ibid.* **43**, 4373 (1991); Z. H. Wang, C. Li, A. J. Epstein, E. M. Scherr, and A. G. MacDiarmid, Phys. Rev. Lett. **66**, 1745 (1991); Z. H. Wang, E. M. Scherr, A. G. MacDiarmid, and A. J. Epstein, Phys. Rev. B **45**, 4190 (1992); J. Joo, Z. Oblakowski, G. Du, J. P. Pouget, E. J. Oh, J. M. Weisinger, Y. Min, A. G. MacDiarmid, and A. J. Epstein, *ibid.* **49**, 2977 (1994); J. Joo, A. J. Epstein, V. N. Prigodin, Y. Min, and A. G. MacDiarmid (unpublished).

[6] M. E. Józefowicz, R. Laversanne, H. H. S. Javadi, A. J. Epstein, J. P. Pouget, X. Tang, and A. G. MacDiarmid, Phys. Rev. B **39**, 12 958 (1989); J. P. Pouget, M. E. Józefowicz, A. J. Epstein, X. Tang, and A. G. MacDiarmid, Macromolecules **24**, 779 (1991).

[7] J. M. Ginder, A. F. Richter, A. G. MacDiarmid, and A. J. Epstein, Solid State Commun. **63**, 97 (1987); A. J. Epstein, J. M. Ginder, F. Zuo, R. W. Bigelow, H. S. Woo, D. B. Tanner, A. F. Richter, W. S. Huang, and A. G. MacDiarmid, Synth. Met. **17**, 433 (1987).

[8] S. Stafström, J. L. Brédas, A. J. Epstein, H. S. Woo, D. B. Tanner, W. S. Huang, and A. G. MacDiarmid, Phys. Rev. Lett. **59**, 1464 (1987).

[9] M. Angelopoulos, G. E. Asturias, S. P. Ermer, A. Ray, E. M. Scherr, A. G. MacDiarmid, M. Akhtar, Z. Kiss, and A. J. Epstein, Mol. Cryst. Liq. Cryst. **160**, 151 (1988).

[10] X. Tang, Y. Sun, and Y. Wei, Makromol. Chem. **9**, 829 (1988).

[11] A. G. MacDiarmid, G. E. Asturias, D. L. Kershner, S. K. Manohar, A. Ray, E. M. Scherr, Y. Sun, X. Tang, and A. J. Epstein, Polym. Prepr. (Am. Chem. Soc. Div. Polym. Chem.) **80**, 147 (1989).

[12] A. G. Green and A. E. Woodhead, J. Chem. Soc. Trans. **97**, 2388 (1910).

[13] A. G. Green and A. E. Woodhead, J. Chem. Soc. Trans. **101**, 1117 (1912).

[14] A. Andreatta, Y. Cao, J. C. Chiang, A. J. Heeger, and P. Smith, Synth. Met. **26**, 383 (1988).

[15] M. Angelopoulos, A. Ray, A. G. MacDiarmid, and A. J. Epstein, Synth. Met. **21**, 21 (1987).

[16] A. G. MacDiarmid, J. M. Weisinger, and A. J. Epstein, Bull Am. Phys. Soc. **38**, 311 (1993); A. G. MacDiarmid and A. J. Epstein, in *Proceedings of the Second Brazillian Polymer Conference, Sao Paulo, Brazil, 1993* (Plenum, New York, 1993), Vol. 1, p. 544.

[17] A. J. Epstein, J. Joo, C. Y. Wu, A. Benatar, C. F. Faust, Jr., J. Zegarski, and A. G. MacDiarmid, in *Intrinsically Conducting Polymers: An Emerging Technology,* edited by M. Aldissi (Kluwer Academic, Dordrecht, 1993), p. 165.

[18] Y. Cao, P. Smith, and A. J. Heeger, Synth. Met. **48**, 91 (1992); Y. Cao and A. J. Heeger, *ibid.* **52**, 193 (1992).

[19] X. Tang, E. M. Scherr, A. G. MacDiarmid, and A. J. Epstein, Bull. Am. Phys. Soc. **34**, 583 (1989); E. M. Scherr, A. G. MacDiarmid, S. K. Manohar, J. G. Masters, Y. Sun, X. Tang, M. A. Druy, P. J. Glatkowski, V. B. Cajibe, J. E. Fischer, K. R. Cromack, M. E. Józefowicz, J. M. Ginder, R. P. McCall, and A. J. Epstein, Synth. Met. **41**, 735 (1991).

[20] K. R. Cromack, M. E. Józefowicz, J. M. Ginder, A. J. Epstein, R. P. McCall, G. Du, J. M. Leng, K. Kim, C. Li, Z. H. Wang, M. A. Druy, P. J. Glatkowski, E. M. Scherr, and A. G. MacDiarmid, Macromolecules **24**, 4157 (1991).

[21] A. P. Monkman and P. Adams, Solid State Commun. **78**, 29 (1991); Synth. Met. **41**, 627 (1991).

[22] A. G. MacDiarmid, J. C. Chiang, A. F. Richter, N. L. D. Somasiri, and A. J. Epstein, in *Conduting Polymers,* edited by L. Alcácer (Reidel, Dordrecht, 1987), p. 105.

[23] A. Ray, G. E. Asturias, D. L. Kershner, A. F. Richter, A. G. MacDiarmid, and A. J. Epstein, Synth Met. **29**, E141 (1989).

[24] Y. Wei, G. W. Jang, K. F. Hsueh, E. M. Scherr, A. G. MacDiarmid, and A. J. Epstein, Polym. Mater. Sci. Eng. **61**, 916 (1989).

[25] Frederick Wooten, *Optical Properties of Solids* (Academic, New York, 1972).

[26] R. P. McCall, J. M. Ginder, J. M. Leng, H. J. Ye, S. K. Manohar, J. G. Masters, G. E. Asturias, A. G. MacDiarmid, and A. J. Epstein, Phys. Rev. B **36**, 5202 (1990).

[27] D. S. Boudreaux, R. R. Chance, J. F. Wolf, L. W. Shacklette, J. L. Brédas, B. Thémas, J. M. André, and R. Silbey, J. Chem. Phys. **85**, 4584 (1986).

[28] C. B. Duke, A. Paton, E. M. Conwell, W. R. Salanek, and I. Lundstrom, J. Chem. Phys. **86**, 3414 (1987).

[29] S. Stafström and J. L. Brédas, Synth. Met. **14**, 297 (1986).

[30] C. B. Duke, E. M. Conwell, and A. Paton, Chem. Phys. Lett. **131**, 82 (1986).

[31] S. Stafström, B. Sjögren, and J. L. Brédas, Synth. Met. **29**, E219 (1989).

[32] B. Sjögren and S. Stafström, J. Chem. Phys. **88**, 3840 (1988).

[33] J. L. Brédas (private communication).

[34] J. M. Leng, R. P. McCall, K. R. Cromack, Y. Sun, S. K. Manohar, A. G. MacDiarmid, and A. J. Epstein, Phys. Rev. B **48**, 15 719 (1993).

[35] A. J. Epstein, R. P. McCall, J. M. Ginder, and A. G. MacDiarmid, in *Spectroscopy of Advanced Materials,* edited by R. J. H. Clark and R. E. Hester (Wiley, Chichester, 1991), Vol. 19, p. 355.

[36] J. M. Ginder and A. J. Epstein, Phys. Rev. B **41**, 10 674 (1990).

[37] David J. Bergman and David Stroud, in *Solid State Physics,* edited by H. Ehrenreich and D. Turnbull (Academic, New York, 1992), Vol. 46, p. 148.

[38] G. Leising, Phys. Rev. B **38**, 10 313 (1988).